Adaptive Calibration for Fusion-based Wireless Sensor Networks

Rui Tan[1] Guoliang Xing[2] Xue Liu[3] Jianguo Yao[3] Zhaohui Yuan[4]
[1]City University of Hong Kong, HKSAR [2]Michigan State University, USA
[3]McGill University, Canada [4]Wuhan University, P.R. China

***Abstract*—Wireless sensor networks (WSNs) are typically composed of low-cost sensors that are deeply integrated with physical environments. As a result, the sensing performance of a WSN is inevitably undermined by various *physical uncertainties*, which include stochastic sensor noises, unpredictable environment changes and dynamics of the monitored phenomenon. Traditional solutions (*e.g.*, sensor calibration and collaborative signal processing) work in an open-loop fashion and hence fail to adapt to these uncertainties after system deployment. In this paper, we propose an *adaptive* system-level calibration approach for a class of sensor networks that employ data fusion to improve system sensing performance. Our approach features a feedback control loop that exploits sensor heterogeneity to deal with the aforementioned uncertainties in calibrating system performance. In contrast to existing heuristic based solutions, our control-theoretical calibration algorithm can ensure provable system stability and convergence. We also systematically analyze the impacts of communication reliability and delay, and propose an optimal routing algorithm that minimizes the impact of packet loss on system stability. Our approach is evaluated by both experiments on a testbed of Tmotes as well as extensive simulations based on data traces gathered from a real vehicle detection experiment. The results demonstrate that our calibration algorithm enables a network to maintain the optimal detection performance in the presence of various system and environmental dynamics.**

I. Introduction

Wireless sensor networks (WSNs) are increasingly deployed in mission-critical applications such as target detection [1], localization [2] and security surveillance [3]. In these applications, low-cost sensors are deeply embedded in physical environments and often suffer significant performance variations. In particular, the sensing performance of a sensor network is greatly affected by stochastic sensor noises, unpredictable environment changes and dynamics of the monitored physical process. In order to achieve desirable system performance, the operational parameters of a network must be dynamically calibrated in response to these uncertainties.

Several approaches have been proposed to deal with the aforementioned uncertainties faced by WSNs. Advanced collaborative signal processing algorithms such as data fusion [4] can mitigate the impact of noise by jointly considering the measurements of multiple sensors. However, these algorithms are not designed to handle hardware biases or environmental dynamics. Sensor calibration [5]–[7] can correct hardware biases by tuning each individual sensor based on ground truth information about physical processes. However, the ground truth information is often unknown or subject to dynamic evolution in reality, which often leads to unpredictable system performance at run time.

In this paper, we exploit the heterogeneity of WSNs to achieve adaptive calibration performance for surveillance WSNs. Many practical WSNs have multiple sensor modalities. For instance, a typical surveillance system [8] has both *low-end* passive infrared sensors and *high-quality* pan-tilt-zoom cameras. Low-end sensors consume less energy but often have limited sensing capability such as high false alarm rate. In contrast, high-quality sensors can yield high-fidelity measurements at the price of high energy consumption. In our calibration approach, low-end sensors collaboratively detect targets through data fusion [4]. When a positive detection consensus is reached by low-end sensors, high-quality sensors are activated to make a high-fidelity detection. The low-end sensors are then iteratively calibrated according to the detection results of high-quality sensors. In particular, the high-quality sensors are allowed to sleep for most of the time and only activated when a possible target is detected by low-end sensors. Such a two-tier calibration framework can significantly reduce system energy consumption while maintaining satisfactory surveillance performance.

Several challenges must be addressed for calibrating the system performance of heterogeneous WSNs. First, the system detection performance is tightly coupled with the measurements of low-end sensors that are often corrupted by random noises from physical environment and sensor hardware. The stochastics in sensor measurements must be carefully considered in order to achieve the optimal detection performance. Second, in an adaptive calibration process, there exist fundamental trade-offs between the system stability and the delay of response to system and environmental dynamics. The trade-offs must be balanced to maintain satisfactory system stability and timeliness. Third, the system calibration performance is inherently impacted by the underlying communication network. An adaptive calibration algorithm must account for various dynamic characteristics of wireless communications, such as link reliability, delay, and routing quality.

We make the following major contributions in this paper.

- We propose a novel approach that exploits sensor heterogeneity for adaptively calibrating the performance of fusion-based WSNs. In our approach, high-quality sensors are activated by low-end sensors only when a possible target is present. The sensing results of high-quality sensors are then fed back to low-end sensors for tuning their performance.
- We formally formulate the problem of adaptive calibration for target detection as a control problem. The system ob-

jective is to maximize the detection performance and adapt to changeable network conditions and physical environments. We develop an adaptive calibration algorithm based on control theory. We also systematically analyze the impacts of communication reliability and delay. Moreover, we propose an optimal routing algorithm that minimizes the impact of packet loss on system stability.
- We implement the adaptive calibration algorithm on a testbed composed of Tmotes [9] and a webcam. We also conduct extensive trace-driven simulations using real data traces collected by 17 sensors in a vehicle detection experiment [10]. The results demonstrate that the calibrated network maintains optimal detection performance in the presence of various system and environmental dynamics.

The rest of this paper is organized as follows. Section II reviews related work. Section III introduces the preliminaries and Section IV formally formulates the adaptive calibration problem. Section V models the system detection performance of a fusion-based WSN. Section VI develops the adaptive calibration algorithm based on control theory. Section VII discusses the impacts of communication performance. Section VIII and IX present the experiment results of testbed and trace-driven simulations, respectively. Section X concludes this paper.

II. Related Work

Sensor calibration is a fundamental problem in WSNs. Early works focus on calibrating individual sensors to output accurate readings. For instance, in [5], each chemical sensor is carefully calibrated in controlled environments to obtain the mapping from its reading to the true value. Recent system-level calibration approaches aim to optimize the overall system performance. In [6], the biases of light sensors are estimated by solving the equations that correlate the sensor biases with the sensor measurements. Similarly, in [7], the operational parameters of ranging sensors are estimated by regression based on pair-wise range measurements. The above approaches calibrate sensors according to known ground truth inputs. In contrast, our approach exploits the sensor heterogeneity and does not require the ground truth inputs.

Feedback control has been widely adopted to improve the adaptability of computing systems and networks [11]. Recently, it is employed to develop various protocols for WSNs, such as MAC-layer [12], energy management [13] and topology control [14] protocols. Different from these works, we develop a control-theoretical calibration algorithm that maximizes the system detection performance of surveillance WSNs under changeable network conditions and physical environments. Data fusion [4] has been proposed as an effective signal processing technique to improve the system detection performance of surveillance applications [3], [15]. Most previous works [4], [16] focus on analyzing the optimal fusion strategies of a given network. In our recent works [17], [18], we investigate the impact of data fusion on coverage and detection delay of WSNs. In this paper, we aim to adaptively calibrate the fusion parameters to increase system sensing performance in the presence of dynamics of environment and monitored phenomenon.

III. Preliminaries

In this section, we present the preliminaries of our work, which include sensor measurement, data fusion and Bayesian detection models.

A. Sensor Measurement Model

We assume that sensors perform detection by measuring the energy of signals, *e.g.*, acoustic signal, emitted by the target. Let s_i denote the signal energy received by sensor i. The signal energy s_i varies with the target and sensor i due to several affecting issues. First, the signal energy s_i depends on the source energy of the target and the signal path loss. The signal path loss is determined by the distance from the target and the physical environments such as terrain. Second, it is affected by the systematic bias of the sensor.

The sensor measurements are contaminated by additive random noises from sensor hardware or environment. Depending on the hypothesis that the target is absent (H_0) or present (H_1), the measurement of sensor i, denoted by y_i, is given by

$$\begin{cases} H_0: & y_i = n_i, \\ H_1: & y_i = s_i + n_i, \end{cases}$$

where n_i is the energy of noise experienced by sensor i. We assume that the noise n_i at each sensor i follows the normal distribution, *i.e.*, $n_i \sim \mathcal{N}(\mu_i, \sigma_i^2)$, where μ_i and σ_i^2 are the mean and variance of n_i, respectively. We assume that the noises, $\{n_i|\forall i\}$, are spatially independent across sensors.

The above stochastic sensor measurement model has been widely adopted in the literature of multi-sensor signal detection [2], [4], [16], [17], [19] and also empirically verified [2], [20]. Many previous works [2], [16], [17], [19] based on the above sensor measurement model assume that the signal energies $\{s_i|\forall i\}$ and noise profiles $\{\mu_i, \sigma_i^2|\forall i\}$ are known *a priori*. However, these parameters are often difficult to estimate and also subject to change due to the dynamics of target and environment. In this paper, we assume that they are unknown to the network.

Table I summarizes the notation used in this paper.

B. Multi-sensor Data Fusion Model

Data fusion [4] has been proposed as an effective signal processing technique to improve the system performance of sensor networks. A sensor network that employs data fusion is often organized into clusters. The cluster head is responsible for making a decision regarding the presence of target by fusing the information gathered by member sensors. As sensors can only carry out limited processing due to resource constraints, we adopt a simple data fusion scheme as follows. The cluster head makes the detection decision according to the sum of measurements reported by member sensors. Such a data fusion model has been widely adopted by previous literature on signal detection [16], [17]. Suppose there are N sensors in a cluster, the sum of measurements, denoted by Y, is given by $Y = \sum_{i=1}^{N} y_i$. Let $\widetilde{H}(Y)$ represent the detection decision rule adopted by the cluster head. Therefore, $\widetilde{H}(Y) \in \{\widetilde{H}_0, \widetilde{H}_1\}$,

TABLE I
SUMMARY OF NOTATION

Symbol	Definition
H_0 / H_1	the ground truth that the target is absent / present
$\widetilde{H}_0$ / $\widetilde{H}_1$	cluster head's decision that the target is absent / present
μ_i, σ_i^2	noise mean and variance of sensor i, respectively
s_i	the signal energy received by sensor i
n_i	noise energy of sensor i, $n_i \sim \mathcal{N}(\mu_i, \sigma_i^2)$
y_i	signal energy measurement of sensor i
N	the number of sensors in the cluster concerned
Y	fused measurement, $Y = \sum_{i=1}^{N} y_i$
μ / σ^2 / S	$\mu = \sum_{i=1}^{N} \mu_i$, $\sigma^2 = \sum_{i=1}^{N} \sigma_i^2$, $S = \sum_{i=1}^{N} s_i$
C_{ij}	the cost of deciding $\widetilde{H}_i$ when the ground truth is H_j
m	the number of detections in a calibration cycle
P_{FL}/P_{ML}	false alarm rate/missing probability of low-end sensors
P_{FH}/P_{MH}	false alarm rate/missing probability of high-quality sensor
P_a	target appearance probability, $P_a = \mathbb{P}(H_1)$
D	the lower bound of target appearance time

where $\widetilde{H}_0$ and $\widetilde{H}_1$ are the detection decisions that the target is absent and present, respectively.

The detection of a target is inherently stochastic due to the random noises in sensor measurements. The *system* detection performance is characterized by two metrics, namely, the false alarm rate (denoted by P_F) and missing probability (denoted by P_M). P_F is the probability of deciding $\widetilde{H}_1$ when *no* target is present, and P_M is the probability of deciding $\widetilde{H}_0$ when a target is present. Formally, $P_F = \mathbb{P}(\widetilde{H}(Y) = \widetilde{H}_1 | H_0)$ and $P_M = \mathbb{P}(\widetilde{H}(Y) = \widetilde{H}_0 | H_1)$.

C. Bayesian Detection Model

Bayesian criterion [21] is a widely adopted decision criterion for detection systems [4]. The objective of Bayesian detection is to minimize the expected cost or risk in making decisions. Under the data fusion model in Section III-B, the Bayesian detection is formally stated as follows. Let $c(\widetilde{H}(Y)|Y)$ denote the expected cost due to making decisions according to the decision rule $\widetilde{H}(Y)$ when the fused measurement is Y. Specifically, $c(\widetilde{H}_0|Y) = C_{00}\mathbb{P}(H_0|Y) + C_{01}\mathbb{P}(H_1|Y)$ and $c(\widetilde{H}_1|Y) = C_{10}\mathbb{P}(H_0|Y) + C_{11}\mathbb{P}(H_1|Y)$, where C_{ij} is the cost of deciding $\widetilde{H}_i$ when the ground truth is H_j and $\mathbb{P}(H_j|Y)$ is the posterior probability of the ground truth H_j when the fused measurement is Y. Note that the costs, *i.e.*, C_{ij}, are constants specified by user. The expected cost over all possible measurements is given by

$$\mathbb{E}[c] = \int_{-\infty}^{\infty} c(\widetilde{H}(Y)|Y) p(Y) \mathrm{d}Y, \tag{1}$$

where $p(Y)$ is the probability density function (PDF) of Y. Note that $p(Y) = p(Y|H_0)\mathbb{P}(H_0) + p(Y|H_1)\mathbb{P}(H_1)$, where $p(Y|H_j)$ is the likelihood given ground truth H_j. The Bayesian detection is the detection rule $\widetilde{H}(Y)$ that minimizes $\mathbb{E}[c]$ [21].

In practice, the costs, *i.e.*, C_{ij}, can be defined according to various system objectives. For instance, by letting $C_{00} = C_{11} = 0$ and $C_{10} = C_{01} = 1$, $\mathbb{E}[c]$ equals the expected probability that the detector makes wrong decisions over all possible measurements [21], *i.e.*, the average error rate. Moreover, by letting C_{ij} be the energy consumed in the operations triggered by deciding $\widetilde{H}_i$ when the ground truth is H_j, $\mathbb{E}[c]$ is the average energy consumed by the system due to detection.

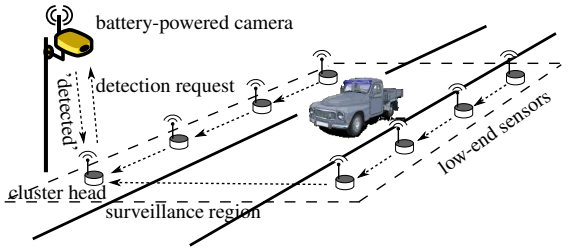

Fig. 1. The illustration of system architecture. The system composed of a number of low-end sensors and a high-quality sensor detects whether a vehicle is present in the rectangular surveillance region.

IV. PROBLEM FORMULATION

This section formulates our problem. Section IV-A presents the network and target models. Section IV-B formally formulates the closed-loop calibration problem. Section IV-C presents the overview of our approach to the problem.

A. Network and Target Models

We assume that a heterogeneous WSN is composed of *low-end* and *high-quality* sensors. The objective is to detect targets that randomly appear. The low-end sensors (*e.g.*, MICA motes) often have low manufacturing cost and energy consumption. However, they usually have limited sensing capability such as high false alarm rate [3]. To improve the system detection performance, the low-end sensors collaboratively detect targets by fusing their measurements as stated in Section III-B. The high-quality sensors (*e.g.*, cameras [8] and active radars [22]) are capable of high-accuracy and complex surveillance such as target tracking and classification. In this paper, they are only required to detect whether a target is present and the detection results are used to calibrate the low-end sensors to achieve desirable detection performance. The high-quality sensors often have higher manufacturing cost and consume more energy. Due to the high cost, we assume that there is only one high-quality sensor in the network. We note that our approach can be easily extended to the scenarios of multiple high-quality sensors where they may fuse their measurements to yield a detection result.

We now illustrate the system architecture using an example. In Fig. 1, a heterogeneous WSN is deployed to detect whether a vehicle is present in the surveillance region. The low-end sensors transmit their measurements to the cluster head through multi-hop paths. The cluster head fuses the received measurements to make a detection decision regarding the presence of the vehicle. The camera can accurately detect the vehicle via image processing techniques. However, the camera often consumes much energy in capturing and processing images. The objective is to calibrate the low-end sensors according to the detection results of the camera such that the detection performance of the system is maximized. Moreover, the system

should be able to adapt to the unpredictable and dynamic changes of the target profiles and physical environments.

Before formally formulating the problem, we make the following assumptions. First, the probability that a target is present at any time instance is P_a which is known or can be estimated from detection history. Second, the target appearance time is lower-bounded by constant D. Third, the false alarm rate and missing probability of the high-quality sensor, denoted by P_{FH} and P_{MH}, are known. For instance, P_{FH} and P_{MH} can be measured via offline experiments. Due to the high accuracy of the high-quality sensor, both P_{FH} and P_{MH} are close to zero.

B. Closed-loop Calibration Problem

The optimal Bayesian detector has been extensively studied in previous literature [4], [21]. We now investigate the optimal detection rule for low-end sensors under the assumptions made in Section III. Suppose there are N low-end sensors. Denote $S = \sum_{i=1}^{N} s_i$, $\mu = \sum_{i=1}^{N} \mu_i$ and $\sigma^2 = \sum_{i=1}^{N} \sigma_i^2$. The optimal detection rule $\widetilde{H}(Y)$ for low-end sensors that minimizes the expected cost $\mathbb{E}[c]$ is given by the following threshold-based decision (the derivation can be found in the appendix):

$$Y \underset{\widetilde{H}(Y)=\widetilde{H}_0}{\overset{\widetilde{H}(Y)=\widetilde{H}_1}{\gtrless}} T_{\text{opt}}, \tag{2}$$

where Y is the sum of the measurements from low-end sensors and the optimal detection threshold T_{opt} is given by

$$T_{\text{opt}} = \frac{\delta\sigma^2}{2S} + \mu + \frac{S}{2}, \tag{3}$$

$$\delta = 2\ln\left(\frac{1-P_a}{P_a} \cdot \frac{C_{10}-C_{00}}{C_{01}-C_{11}}\right). \tag{4}$$

Note that δ is a known constant as long as P_a and $\{C_{ij}|i,j \in \{0,1\}\}$ are given.

In the above optimal detection rule, the optimal detection threshold T_{opt} is often unknown and cannot be easily estimated in practice. First, μ and σ^2 are the sums of noise means and variances at all low-end sensors, respectively. Although the noise means and variances can be estimated offline (*e.g.*, in laboratory), they may change at run time. For instance, the noise profiles would change with environmental conditions (*e.g.*, wind) as well as the electronic noise in sensor hardware affected by ambient temperatures. Second, S is the sum of signals received by low-end sensors and hence is affected by the source energy and physical position of the target. However, both the source energy and position of the target are unknown and changeable in practice. Moreover, if the ground truth information is not available, the detection approaches based on the μ, σ^2 and S that are estimated from noisy measurements will lead to circular reasoning. As a result, implementing the optimal detection rule based on unknown μ, σ^2 and S is largely unpractical in practice.

In this paper, we exploit sensor heterogeneity to overcome the difficulties caused by the unknown variables μ, σ^2 and S. As the high-quality sensor can detect the target accurately, the detection results can be fed back to calibrate the low-end sensors when the target profiles and environment conditions have changed. Specifically, the detection threshold at the cluster head, denoted by T, is iteratively calibrated according to the feedback of the high-quality sensor, such that the network achieves the optimal detection performance. Our problem is formally formulated as follows.

Problem 1. *To find a* stable *and* converging *calibration algorithm for the detection threshold T at the cluster head based on the feedback of high-quality sensor, such that the expected cost due to detections,* i.e.*, $\mathbb{E}[c]$ which is given by (1), is minimized.*

We define *stability* and *convergence* based on control theories [23] as follows. The closed-loop system is *stable* if the system output $\mathbb{E}[c]$ is bounded given bounded inputs μ, σ^2 and S. Furthermore, the system *converges* if the system output $\mathbb{E}[c]$ converges to its theoretical minimum if all inputs are fixed. Moreover, in order to improve the real-time performance of the system, we expect that the output $\mathbb{E}[c]$ converges as soon as possible when the inputs have changed.

C. Approach Overview

Feedback control has been widely employed to improve the system adaptability of networks [11]. In Problem 1, the system objective is to adapt to the unpredictable and dynamic changes of target profiles and physical environments. We face several major challenges in implementing the closed-loop calibration. First, the relationship between the detection performance of low-end sensors and their stochastic measurements must be carefully considered to minimize the expected cost $\mathbb{E}[c]$. Second, the high-quality sensor should sleep for most of the time when no target is present due to its high energy consumption. To address these challenges, we propose a calibration approach that features feedback control loop to adaptively calibrate the detection threshold T, where the controller is implemented by the calibration algorithm located at the cluster head. The overview of our approach is as follows.

The detection threshold T is calibrated iteratively for every *calibration cycle*. Each calibration cycle comprises a number of detections. In each detection, the cluster head fuses the measurements received from the low-end sensors to make a detection decision by comparing against the current detection threshold T. Only if the cluster head makes a positive detection decision, the high-quality sensor is activated to make a detection and reports its decision to the cluster head. Such an on-demand activation scheme enables the high-quality sensor to sleep when no target is present. At the end of each calibration cycle, the cluster head estimates the detection performance of low-end sensors, which is characterized by the false alarm rate and missing probability, according to the detection history and the feedback of the high-quality sensor. The cluster head then calibrates the detection threshold T according to the difference between the estimated and the optimal detection performances.

In the rest of this paper, we first derive the closed-form expressions of the false alarm rate and missing probability of low-end sensors in Section V. We then develop an adaptive

calibration algorithm based on feedback control theory in Section VI. Moreover, we analyze the impacts of communication performance on our algorithm in Section VII.

V. Performance Modeling

In this section, we first derive the theoretical expressions of the system false alarm rate and missing probability of low-end sensors. We then derive the estimators of the two probabilities based on the feedback of the high-quality sensor.

A. Detection Performance of Low-end Sensors

We now derive the false alarm rate and missing probability of low-end sensors. Recall the distributions of $Y|H_0$ and $Y|H_1$ that are derived in the appendix, *i.e.*, $Y|H_0 \sim \mathcal{N}(\mu, \sigma^2)$ and $Y|H_1 \sim \mathcal{N}(\mu + S, \sigma^2)$. The system false alarm rate and missing probability of low-end sensors (denoted by P_{FL} and P_{ML}) are given by $P_{FL} = \mathbb{P}(Y \geq T|H_0) = Q\left(\frac{T-\mu}{\sigma}\right)$ and $P_{ML} = \mathbb{P}(Y \leq T|H_1) = Q\left(-\frac{T-\mu-S}{\sigma}\right)$, respectively, where $Q(\cdot)$ is the complementary cumulative distribution function of the standard normal distribution, *i.e.*, $Q(x) = \int_{t=x}^{+\infty} \frac{1}{\sqrt{2\pi}} \exp\left(-\frac{t^2}{2}\right) \mathrm{d}t$. We now investigate the relationship between P_{FL} and P_{ML} when the expected cost $\mathbb{E}[c]$ is minimized which is the objective of Problem 1. Let $Q^{-1}(\cdot)$ denote the inverse function of $Q(\cdot)$. We have the following lemma.

Lemma 1. *The expected cost $\mathbb{E}[c]$ is minimized if and only if $V = \delta$, where $V = \left(Q^{-1}(P_{FL})\right)^2 - \left(Q^{-1}(P_{ML})\right)^2$ and δ is given by (4).*

Proof: From the expressions of P_{FL} and P_{ML}, we have

$$\begin{aligned} V &= \left(Q^{-1}(P_{FL})\right)^2 - \left(Q^{-1}(P_{ML})\right)^2 \\ &= \left(\frac{T-\mu}{\sigma}\right)^2 - \left(-\frac{T-\mu-S}{\sigma}\right)^2 \\ &= \frac{2S}{\sigma^2} \cdot T - \frac{2\mu S + S^2}{\sigma^2}. \end{aligned} \tag{5}$$

As discussed in Section IV-B, $\mathbb{E}[c]$ is minimized if and only if $T = T_{\text{opt}}$, where T_{opt} is given by (3). By replacing T in (5) with T_{opt}, we have $V = \delta$. Moreover, as V is a linear function of T, $\mathbb{E}[c]$ is minimized if and only if $V = \delta$. ∎

We note that δ is a known constant which is independent of the unknown variables μ, σ^2 and S. From Lemma 1, Problem 1 can be reduced to the following problem.

Problem 2. *To find the* stable *and* converging *calibration algorithm for the detection threshold T at the cluster head based on the feedback of high-quality sensor, such that $V = \delta$, where $V = \left(Q^{-1}(P_{FL})\right)^2 - \left(Q^{-1}(P_{ML})\right)^2$ and δ is given by (4).*

In Section VI, we will develop a calibration algorithm based on feedback control theory to solve Problem 2.

B. Feedback of High-quality Sensor

The objective of system detection performance defined in Problem 2 is to ensure $V = \delta$ where V is computed by P_{FL} and P_{ML}. In this section, we derive the estimators of P_{FL} and P_{ML} based on the detection history of low-end sensors and the feedback of the high-quality sensor.

Suppose each calibration cycle comprises m detections. The low-end sensors fuse their measurements to make a detection for every D seconds such that each sensor can sample at least one measurement when the target is present. Note that D is the lower bound of target appearance time. At the end of a calibration cycle, the cluster head counts the numbers of positive and negative decisions made by the high-quality sensor and estimates P_{FL} and P_{ML} based on the counts. We note that the high-quality sensor may make wrong detection decisions where the false alarm rate and missing probability are P_{FH} and P_{MH}, respectively, as assumed in Section IV-A. Therefore, our estimators account for the inaccuracy of the high-quality sensor.

We define the following notation subject to a calibration cycle: 1) n_{f1} and n_{d1} are the numbers of false alarms and correct detections made by the cluster head, respectively, which are unknown; 2) n_{f2} and n_{d2} are the numbers of positive decisions made by the cluster head but regarded to be false alarms and correct detections by the high-quality sensor, respectively, which can be counted by the cluster head. We have the following equations,

$$n_{f2} \simeq n_{f1}(1 - P_{FH}) + n_{d1} P_{MH}, \tag{6}$$

$$n_{d2} \simeq n_{f1} P_{FH} + n_{d1}(1 - P_{MH}). \tag{7}$$

In (6), $n_{f1}(1 - P_{FH})$ represents the number of false alarms that are correctly identified by the high-quality sensor, and $n_{d1} P_{MH}$ represents the number of correct detections that are wrongly classified as false alarms. In (7), $n_{f1} P_{FH}$ represents the number of false alarms that are wrongly classified as correct detections, and $n_{d1}(1 - P_{MH})$ represents the number of detections that are correctly identified. From (6) and (7), the unknown n_{f1} and n_{d1} can be estimated as

$$n_{f1} \simeq \frac{n_{f2}(1 - P_{MH}) - n_{d2} P_{MH}}{1 - P_{FH} - P_{MH}},$$

$$n_{d1} \simeq \frac{n_{d2}(1 - P_{FH}) - n_{f2} P_{FH}}{1 - P_{FH} - P_{MH}}.$$

Therefore, the estimates of P_{FL} and P_{ML}, denoted by $\widetilde{P}_{FL}$ and $\widetilde{P}_{ML}$, respectively, are given by

$$\widetilde{P}_{FL} = \frac{n_{f1}}{m - m \cdot P_a}, \quad \widetilde{P}_{ML} = \frac{m \cdot P_a - n_{d1}}{m \cdot P_a}. \tag{8}$$

Note that $m \cdot P_a$ is the expected number of target appearances in a calibration cycle. The major errors of the above estimates are caused by the difference between the mean value $m \cdot P_a$ and the true number of target appearances which is a binomial random variable. The relative estimation errors of (8) are $\mathcal{O}\left(\frac{1}{\sqrt{m}}\right)$. The error analysis is omitted due to space limit and can be found in [24]. Hence, we can choose m to achieve any required estimation accuracy [24]. The impact of m on the calibration performance is also evaluated in Section IX.

VI. Adaptive Calibration Algorithm

In this section, we first derive the control law to solve Problem 2 based on feedback control theory. We then implement the control law as an adaptive calibration algorithm.

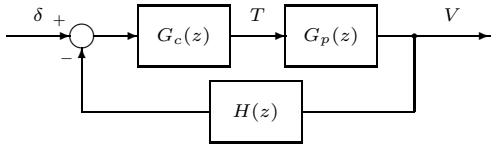

Fig. 2. The closed-loop system for minimizing $\mathbb{E}[c]$, where $G_c(z)$, $G_p(z)$ and $H(z)$ represent the transfer functions of the calibration algorithm, the network of low-end sensors and the feedback of the high-quality sensor, respectively.

A. Control Law

The performance objective of Problem 2 is to ensure $V = \delta$, where V is a function of the detection threshold T given by (5) and can be estimated based on the feedback of the high-quality sensor as discussed in Section V-B. Moreover, the detection threshold T is calibrated for every calibration cycle. Therefore, Problem 2 is a typical discrete-time control problem [23], in which δ is the *reference*, T is the *control input* and V is the *controlled variable*. The block diagram of the feedback control loop is shown in Fig. 2, where $G_c(z)$, $G_p(z)$ and $H(z)$ represent the transfer functions of the calibration algorithm (*i.e.*, controller), the network of low-end sensors and the feedback of the high-quality sensor, respectively.

We now derive the expressions of $G_p(z)$ and $H(z)$, and design $G_c(z)$ to solve Problem 2. By taking z-transform [23] to (5), we get the transfer function $G_p(z)$ as $G_p(z) = \frac{2S}{\sigma^2}$. At the end of a calibration cycle, the cluster head estimates V based on the feedback of the high-quality sensor as discussed in Section V-B. Accordingly, the feedback of the high-quality sensor will take effect in the next calibration cycle. Therefore, the $H(z)$ has a component of z^{-1} that represents a delay of one calibration cycle. As discussed in Section V-B, we can ignore the inaccuracy in estimating V if m is large. Hence, $H(z) = z^{-1}$. As the system to be controlled, *i.e.*, $G_p(z)$, is a zero-order system, a first-order controller is sufficient to achieve the stability and convergence of the closed-loop system [23]. Hence, we let $G_c(z)$ be

$$G_c(z) = \frac{a}{1 - b \cdot z^{-1}}, \tag{9}$$

where $a > 0$ and $b > 0$. The coefficients a and b should be chosen to ensure system stability and convergence. In Section VI-B, we will discuss how to determine a and b based on stability and convergence analyses.

B. Stability and Convergence Analyses

We first analyze the system stability. The closed-loop transfer function, denoted by $T_c(z)$, is given by

$$T_c(z) = \frac{G_c(z)G_p(z)}{1 + G_c(z)G_p(z)H(z)} = \frac{\frac{2aS}{\sigma^2} \cdot z}{z - \left(b - \frac{2aS}{\sigma^2}\right)}.$$

The closed-loop system has a pole at $z = b - \frac{2aS}{\sigma^2}$. From control theory [23], if the pole is within the unit circle centered at the origin, *i.e.*, $|b - \frac{2aS}{\sigma^2}| < 1$, the system is stable. Therefore, the sufficient condition for stability is $\frac{\sigma^2}{2S}(b-1) < a < \frac{\sigma^2}{2S}(b+1)$.

We then analyze the steady-state error of the system. The open-loop transfer function, denoted by $T_o(z)$, is given by

$$T_o(z) = G_c(z)G_p(z)H(z) = \frac{2aS}{\sigma^2(z-b)}.$$

By letting $b = 1$, the system is a type I system [23], of which the controlled variable V can converge to the reference δ provided that the system is stable. Therefore, by replacing b with 1, the condition for both stability and convergence is $0 < a < \frac{\sigma^2}{S}$. Accordingly, only a is left to be determined.

Finally, we discuss the transient response of the system, which characterizes how fast the closed-loop system converges. There exists a fundamental trade-off between the stability and transient response performance [23]. Particularly for our problem, the system converges faster for larger a at the price of worse system stability. Therefore, the best setting for a is a value close to the upper bound $\frac{\sigma^2}{S}$. However, σ^2 and S are often unknown and changeable at run time as discussed in Section IV-B. We now propose an approach to adaptively estimate the upper bound $\frac{\sigma^2}{S}$. The details are as follows.

From (5), the control input T and the controlled variable V have a linear relationship with slope of $K = \frac{2S}{\sigma^2}$. We employ the exponential moving average [25] to estimate and update the slope K. Specifically, in the k^{th} calibration cycle, the slope K is estimated as $K = \frac{V[k-1]-V[k-2]}{T[k-1]-T[k-2]}$, where $T[k-1]$ is the detection threshold set by the calibration algorithm in the $(k-1)^{\text{th}}$ calibration cycle, and $V[k-1]$ is the corresponding output of low-end sensors. We note that $V[k-1]$ is obtained in the k^{th} calibration cycle due to the delay of feedback. The exponential moving average of K in the k^{th} calibration cycle, denoted by $\overline{K}[k]$, is updated by $\overline{K}[k] = (1-\alpha) \cdot \overline{K}[k-1] + \alpha \cdot K$, where α is a weight in $(0, 1)$. Note that the moving average $\overline{K}$ can quickly adapt to the change of K by setting a large α. However, doing so reduces the algorithm robustness to errors such as the inaccuracy in estimating V. The upper bound $\frac{\sigma^2}{S}$ is estimated as $\frac{\sigma^2}{S} = \frac{2}{\overline{K}[k]}$ and a is set to be $\beta \cdot \frac{2}{\overline{K}[k]}$, where β is a coefficient in $(0, 1)$. Note that β is set to be 0.5 in the experiments conducted in this paper. The $\overline{K}[0]$ can be set to be a large enough value such that the system is stable initially.

C. Adaptive Calibration Algorithm

In this section, we implement the control law derived in Section VI-A in time domain. According to Fig. 2, we have $G_c(z) = \frac{T(z)}{\delta - H(z)V(z)}$. By replacing $G_c(z)$ with (9) and $H(z) = z^{-1}$, we have $T(z) = b \cdot z^{-1}T(z) + a \cdot \left(\delta - z^{-1}V(z)\right)$ and its implementation in time domain is $T[k] = b \cdot T[k-1] + a \cdot (\delta - V[k-1])$, where $V[k-1] = \left(Q^{-1}(\widetilde{P}_{FL})\right)^2 - \left(Q^{-1}(\widetilde{P}_{ML})\right)^2$, $T[k-1]$ and $T[k]$ are the detection thresholds in the $(k-1)^{\text{th}}$ and k^{th} calibration cycle, respectively. The estimates $\widetilde{P}_{FL}$ and $\widetilde{P}_{ML}$ are computed using (8) when the detection threshold is $T[k-1]$. As discussed in Section VI-B, $b = 1$ and a is updated for each calibration cycle to ensure system stability and convergence.

VII. Impact of Communication Performance

The adaptive calibration algorithm in Section VI is impacted by communication performance. In this section, we investigate

the impacts caused by packet loss and feedback delay.

A. Packet Loss and Optimal Routing Algorithm

In this section, we first analyze the impact of packet loss in the wireless communication among low-end sensors, and then propose an optimal routing algorithm to minimize the impact. From the analysis in Section VI-A, the system stability is affected by the upper bound $\frac{\sigma^2}{S}$. In the case of stochastic packet loss, both the aggregated signal energies and noise variances, *i.e.*, S and σ^2, can change rapidly. The closed-loop system can become unstable due to the rapid changes of S and σ^2. We study the impact of packet loss by investigating the relative deviations of S and σ^2, which characterize the magnitude of changes caused by stochastic packet loss. Let p_i denote the end-to-end packet reception rate (PRR) of the multi-hop path from sensor i to the cluster head. We assume that $p_i \in [0.5, 1]$. Let $u_i \in \{0, 1\}$ denote the packet delivery state of sensor i in a transmission, which is a Bernoulli random variable with success probability of p_i. In the presence of packet loss, $S = \sum_{i=1}^{N} s_i u_i$. We assume that s_i has non-zero lower and upper bounds, denoted by $s_{\min}$ and $s_{\max}$, respectively. Hence, we have $\mathbb{E}[S] = \sum_{i=1}^{N} s_i \mathbb{E}[u_i] = \sum_{i=1}^{N} s_i p_i \geq \frac{N \cdot s_{\min}}{2}$ and $\mathrm{Var}[S] = \sum_{i=1}^{N} s_i^2 \mathrm{Var}[u_i] = \sum_{i=1}^{N} s_i^2 p_i (1 - p_i) \leq \frac{N \cdot s_{\max}^2}{4}$. The relative standard deviation (RSD) [25] of S satisfies $\mathrm{RSD}(S) = \frac{\sqrt{\mathrm{Var}[S]}}{\mathbb{E}[S]} \leq \frac{s_{\max}}{s_{\min}} \cdot \frac{1}{\sqrt{N}}$, *i.e.*, $\mathrm{RSD}(S) = \mathcal{O}\left(\frac{1}{\sqrt{N}}\right)$. Therefore, the impact of packet loss can be mitigated by deploying more low-end sensors. The derivation of $\mathrm{RSD}(\sigma^2)$ is similar and hence omitted here.

We now propose an optimal routing algorithm that minimizes $\mathrm{RSD}(S)$. As $\frac{\partial \mathbb{E}[S]}{\partial p_i} > 0$ and $\frac{\partial \mathrm{Var}[S]}{\partial p_i} \leq 0$ for $p_i \in [0.5, 1]$, $\frac{\partial \mathrm{RSD}(S)}{\partial p_i} \leq 0$. Therefore, $\mathrm{RSD}(S)$ is minimized when each p_i is maximized separately. Let R_i denote the routing path from sensor i to the cluster head and $p(h)$ denote the PRR of hop $h \in R_i$. Accordingly, $p_i = \prod_{\forall h \in R_i} p(h)$ and the optimal routing path that maximizes p_i is given by $\mathrm{argmin}_{R_i} \sum_{\forall h \in R_i} -\log p(h)$, *i.e.*, the shortest path from sensor i to the cluster head where the cost of hop h is $-\log p(h)$. The evaluation of the impact of packet loss as well as routing algorithms on the performance of the calibration algorithm can be found in a technical report [24].

B. Impact of Feedback Delay

In this section, we analyze the impact of feedback delay on system stability. Suppose the feedback is delayed for d calibration cycles where d is an unknown integer. Therefore, the transfer function of the feedback is $H(z) = z^{-d}$. Several practical issues can attribute to the feedback delay, such as the communication delay due to the low duty cycle of sensors. We adopt a widely used technique called the Jury test [23] to analyze the stability of our algorithm. The details are omitted due to space limit and can be found in [24]. Fig. 3 plots the regions of a in (9) for system stability when d is from 1 to 5. We can see from the figure that the stability condition becomes more critical for larger d. This is consistent with the intuition in control theory that the system stability decreases with the delay in the closed-loop. The evaluation of the impact of d can be found in a technical report [24]. The result shows that the feedback delay has little impact on the performance of our calibration algorithm when d is up to 10.

VIII. Testbed Experiments

To evaluate the performance of our adaptive calibration approach, we have conducted both experiments on a testbed of Tmotes as well as extensive trace-driven simulations based on real data traces. We first present the testbed experiments in this section and then the trace-driven simulations in Section IX.

A. Experiment Methodology and Settings

In our experiments, five Tmotes [9] are attached against the LCD screen of a desktop computer to detect a light spot displayed on the LCD. The light spot simulates the target that randomly appears, and its display is controlled by a program. We note that such an experimental methodology is also employed in previous works [26]. The system objective is to adapt to the intensity change of the light spot that randomly appears in each time slot with a probability of $P_a = 50\%$. The length of a time slot is one second. The motes measure light intensity for every 250 milliseconds via the on-board Hamamatsu S1087-01 light sensors [9] and transmit the measurements to the sink node that is connected to a laptop computer. Note that the motes are not synchronized. NesC language is used to program the motes, and Java is used to implement the calibration algorithms that run on the laptop. The sink fuses the readings received within every 250 milliseconds and detects the light spot. A webcam is attached against the LCD and used as the high-quality sensor. When the webcam is triggered by the sink to make a detection, it computes the average intensity over all pixels and makes the detection decision by comparing against a threshold. The threshold is set to be 175 in our experiments. The webcam's false alarm rate and missing probability, *i.e.*, P_{FH} and P_{MH}, are 3.3% and 1.4%, respectively, which are estimated offline. The length of a calibration cycle, *i.e.*, m, is 200 detections. The detection threshold T at the sink is initially set to be zero. We let $C_{00} = C_{11} = 0$ and $C_{10} = C_{01} = 1$. Hence, the cost metric given by (1) is the average error rate of the motes, which is denoted by P_E.

We employ a *heuristic* calibration approach as the baseline, in which the webcam is also activated to make a detection when the cluster head makes a positive decision. The details of the heuristic approach are as follows. Let $\widetilde{H}_0'$ and $\widetilde{H}_1'$ represent the negative and positive detection decisions of the webcam, respectively. The mean and variance of the fused noise, *i.e.*, μ and σ^2, are estimated as $\mathbb{E}[Y|\widetilde{H}_0 \vee (\widetilde{H}_1 \wedge \widetilde{H}_0')]$ and $\mathrm{Var}[Y|\widetilde{H}_0 \vee (\widetilde{H}_1 \wedge \widetilde{H}_0')]$, respectively. The aggregated signal energies is estimated as $S = \mathbb{E}[Y|\widetilde{H}_1 \wedge \widetilde{H}_1'] - \mu$. The detection threshold is then set according to the optimal formula (3) with the estimated S, μ and σ^2. The heuristic calibration approach is a typical way to use the feedback of the high-quality sensor. However, it does not exploit the relationship between the detection performance of low-end sensors and their stochastic measurements.

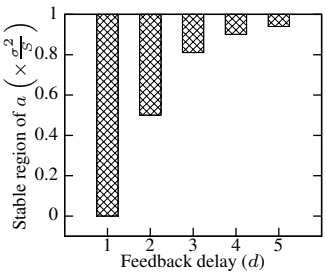

Fig. 3. The region of a for system stability under various d.

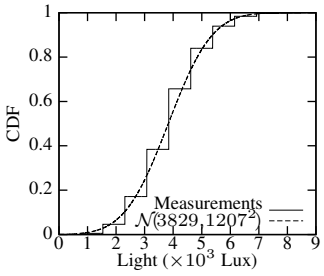

Fig. 4. The CDF of the fused readings from 5 motes.

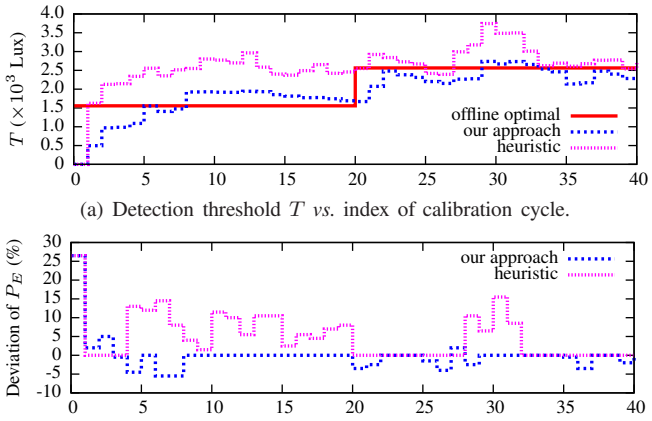

(a) Detection threshold T *vs.* index of calibration cycle.

(b) Deviation of P_E *vs.* index of calibration cycle.

Fig. 5. Convergence of various calibration approaches.

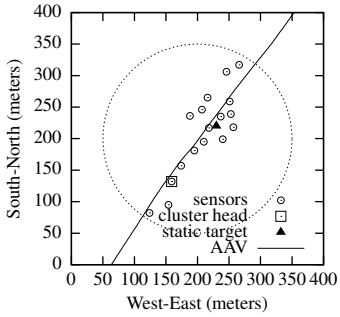

Fig. 6. Sensor deployment and the trajectory of AAV [10].

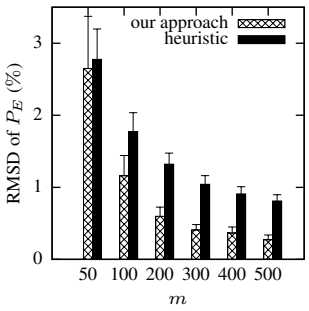

Fig. 7. The RMSD of P_E with respect to the offline optimal approach *vs.* m.

B. Experiment Results

We first evaluate the sensor measurements. Fig. 4 plots the cumulative distribution functions (CDFs) of the fused measurement when the light spot is present as well as the normal distribution $\mathcal{N}(3829, 1207^2)$, respectively. We note that the fused measurement is a discrete random variable. We can see from Fig. 4 that the distribution of the fused measurement can be approximated by the normal distribution, which is consistent with the assumptions in Section III.

We then evaluate the convergence of the calibration approaches. Fig. 5(a) plots the evolution of the detection thresholds calibrated by various approaches. The *offline optimal* approach computes the optimal detection threshold using (3) based on the S, μ and σ^2 that are estimated in extra offline experiments. Note that the offline optimal approach is unpractical in practice as discussed in Section IV-B. At the 20^{th} calibration cycle, we increase the intensity of the light spot to evaluate the adaptability of the calibration approaches. As P_E is the cost metric, Fig. 5(b) plots the deviation of P_E from that of the offline optimal approach. From Fig. 5(a) and 5(b), we can see that our approach converges to the optimal results after 8 calibration cycles. Moreover, our approach can response to the target change within 3 calibration cycles. In contrast, the heuristic approach has considerably large deviations from the optimal results. Specifically, in Fig. 5(a), the average relative errors of our approach and the heuristic approach after the 10^{th} calibration cycle are 12.8% and 30.5%, respectively.

IX. Trace-driven Simulations

A. Simulation Methodology and Settings

We use the real data traces collected in the DARPA SensIT vehicle detection experiment [10], where 75 WINS NG 2.0 nodes are deployed to detect Amphibious Assault Vehicles (AAVs) driving through a road section. We refer to [10] for detailed setup of the experiment. The dataset used in our simulations includes the ground truth data and the acoustic time series recorded by 17 nodes at a frequency of 4960 Hz. The ground truth data include the positions of sensors and the trajectory of the AAV recorded by a GPS device. Fig. 6 [10] shows the sensor deployment and the trajectory of an AAV run. As the AAV is moving, the data traces cannot be directly used to evaluate our calibration approach in detecting static target. In the simulations, we assume that the target appears at a fixed location shown in Fig. 6. A sensor's measurement is set to be the real measurement when the AAV is closest to the fixed location. Besides the case of static target, we also evaluate our approach in detecting moving target. The AAV is regarded to be present when it is in the circular region shown in Fig. 6. As it often takes tens of seconds for the AAV to drive through the road section in Fig. 6, the sampling period of the sensors, *i.e.*, D, is set to be 15 seconds in the simulations. The target appearance probability P_a is set to be 25%. As there is no extra high-quality sensor such as camera in the SensIT experiment, we use a pseudo camera in the simulations, which generates random detection results based on the ground truth data. The pseudo camera's false alarm rate and missing probability, *i.e.*, P_{FH} and P_{MH}, are both set to be 1%.

B. Simulation Results

In the first set of simulations, we evaluate the performance of our calibration approach in detecting static and moving targets. Fig. 8(a) plots the detection thresholds calibrated by various approaches in detecting static targets with changing noise level. The noise standard deviation of each sensor, *i.e.*, σ_i, decreases by 4×10^{-4} in each calibration cycle from the 10^{th} calibration cycle. Fig. 8(b) plots the results of detecting moving targets. Note that calibrating the sensors for detecting moving target is challenging as the aggregated signal energies, *i.e.*, S, significantly varies when the target is at different locations. From the figures, we can see that our approach converges to the optimal results after 10 calibration cycles and can adapt to

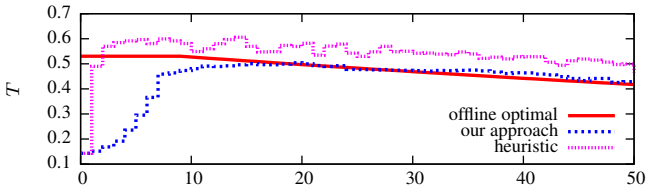

(a) Static target, changing noise level.

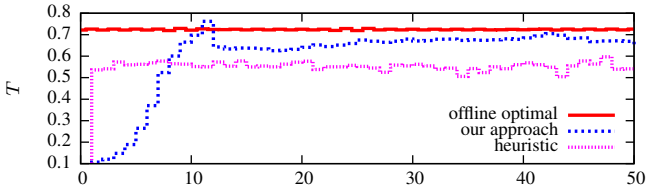

(b) Moving target, constant noise level.

Fig. 8. Detection threshold T *vs.* index of calibration cycle.

changing noise level as well as moving target. Although the heuristic approach has short rise time, it has considerably large steady-state error.

From the error analysis in Section V-B, the number of detections in a calibration cycle, *i.e.*, m, affects the accuracy of feedback. The second set of simulations evaluate the impact of m on the performance of our calibration algorithm. We employ the root mean square deviation (RMSD) of P_E with respect to the offline optimal approach as the performance metric. Specifically, $\mathrm{RMSD}(P_E) = \sqrt{\mathbb{E}[(P_E - P_{E,\mathrm{opt}})^2]}$, where $P_{E,\mathrm{opt}}$ is the average error rate of the offline optimal approach. Fig. 7 plots the RMSD of P_E versus m. The system shows better convergence for larger m, which is consistent with our analysis in Section V-B. Moreover, our approach yields smaller RMSD of P_E than the heuristic approach under a wide range of m.

X. Conclusion

The sensing performance of a WSN is inevitably undermined by the physical uncertainties from environment and the monitored phenomenon. In this paper, we propose an adaptive calibration approach that exploits sensor heterogeneity to deal with these uncertainties. We develop a control-theoretical calibration algorithm that ensures provable system stability and convergence. Our algorithm accounts for various communication issues such as packet loss, delay, and routing quality. The experiment results on a testbed of Tmotes as well as extensive trace-driven simulations demonstrate that the calibrated network maintains the optimal detection performance in the presence of various system and environmental dynamics.

Acknowledgement

The work described in this paper was partially supported by Michigan State University under grant 08-IRGP-1624, and Canadian NSERC Discovery Grant 341823-07, NSERC Strategic Grant STPGP 364910-08, and FQRNT grant 2010-NC-131844.

References

[1] D. Li, K. Wong, Y.-H. Hu, and A. Sayeed, "Detection, classification and tracking of targets in distributed sensor networks," *IEEE Signal Process. Mag.*, vol. 19(2), 2002.

[2] D. Li and Y.-H. Hu, "Energy based collaborative source localization using acoustic micro-sensor array," *EUROSIP Journal on Applied Signal Processing*, no. 4, 2003.

[3] T. He, S. Krishnamurthy, J. A. Stankovic, T. Abdelzaher, L. Luo, R. Stoleru, T. Yan, L. Gu, J. Hui, and B. Krogh, "Energy-efficient surveillance system using wireless sensor networks," in *MobiSys*, 2004.

[4] P. K. Varshney, *Distributed Detection and Data Fusion*. Springer, 1996.

[5] N. Ramanathan, L. Balzano, M. Burt, D. Estrin, T. Harmon, C. Harvey, J. Jay, E. Kohler, S. Rothenberg, and M. Srivastava, "Rapid deployment with confidence: Calibration and fault detection in environmental sensor networks," Center for Embedded Networked Sensing, Tech. Rep., 2006.

[6] J. Feng, S. Megerian, and M. Potkonjak, "Model-based calibration for sensor networks," in *IEEE Sensors*, 2003.

[7] K. Whitehouse and D. Culler, "Calibration as parameter estimation in sensor networks," in *WSNA*, 2002.

[8] C. Wren, U. Erdem, and A. Azarbayejani, "Functional calibration for pan-tilt-zoom cameras in hybrid sensor networks," *Multimedia Systems*, vol. 12, no. 3, 2006.

[9] Moteiv Corp., "Tmote sky datasheet."

[10] M. Duarte and Y.-H. Hu, "Vehicle classification in distributed sensor networks," *J. Parallel and Distributed Computing*, vol. 64(7), 2004.

[11] T. Adbelzaher, Y. Diao, J. L. Hellerstein, C. Lu, and X. Zhu, *Performance Modeling and Engineering*. Springer, 2008, ch. Introduction to Control Theory and its Application to Computing Systems, SIGMETRICS'08.

[12] H. Le, D. Henriksson, and T. Abdelzaher, "A control theory approach to throughput optimization in multi-channel collection sensor networks," in *IPSN*, 2007.

[13] C. Vigorito, D. Ganesan, and A. Barto, "Adaptive control of duty cycling in energy-harvesting wireless sensor networks," in *SECON*, 2007.

[14] L. Shi, K. Johansson, and R. Murray, "Change sensor topology when needed: How to efficiently use system resources in control and estimation over wireless networks," in *IEEE CDC*, 2007.

[15] M. Duarte and Y.-H. Hu, "Distance based decision fusion in a distributed wireless sensor network," in *IPSN*, 2003.

[16] T. Clouqueur, K. K. Saluja, and P. Ramanathan, "Fault tolerance in collaborative sensor networks for target detection," *IEEE Trans. Comput.*, vol. 53(3), 2004.

[17] G. Xing, R. Tan, B. Liu, J. Wang, X. Jia, and C.-W. Yi, "Data fusion improves the coverage of wireless sensor networks," in *MobiCom*, 2009.

[18] R. Tan, G. Xing, B. Liu, and J. Wang, "Impact of data fusion on real-time detection in sensor networks," in *RTSS*, 2009.

[19] X. Sheng and Y.-H. Hu, "Maximum likelihood multiple-source localization using acoustic energy measurements with wireless sensor networks," *IEEE Trans. Signal Process.*, vol. 53(1), 2005.

[20] M. Hata, "Empirical formula for propagation loss in land mobile radio services," *IEEE Trans. Veh. Technol.*, vol. 29, 1980.

[21] R. Duda, P. Hart, and D. Stork, *Pattern Classification*. Wiley, 2001.

[22] P. Dutta, A. Arora, and S. Bibyk, "Towards radar-enabled sensor networks," in *IPSN*, 2006.

[23] K. Ogata, *Discrete-time control systems*. Prentice-Hall, 1995.

[24] R. Tan, G. Xing, X. Liu, J. Yao, and Z. Yuan, "Adaptive calibration for fusion-based wireless sensor networks," City University of Hong Kong, Tech. Rep., 2009, http://www.cs.cityu.edu.hk/~tanrui/pub/camdetect.pdf.

[25] NIST/SEMATECH, *e-Handbook of Statistical Methods*. National Institute of Standards and Technology.

[26] J. Hwang, T. He, and Y. Kim, "Exploring in-situ sensing irregularity in wireless sensor networks," in *SenSys*, 2007.

Appendix

The optimal decision rule $\widetilde{H}(Y)$ that minimizes $\mathbb{E}[c]$ is given by the likelihood ratio test [21]: $\frac{p(Y|H_1)}{p(Y|H_0)} \underset{\widetilde{H}(Y)=\widetilde{H}_0}{\overset{\widetilde{H}(Y)=\widetilde{H}_1}{\gtrless}} \frac{\mathbb{P}(H_0)}{\mathbb{P}(H_1)} \cdot \frac{C_{10}-C_{00}}{C_{01}-C_{11}}$.

We now derive the likelihoods $p(Y|H_0)$ and $p(Y|H_1)$. When the target is present, $Y|H_0 = \sum_{i=1}^{N} n_i \sim \mathcal{N}\left(\mu, \sigma^2\right)$. When the target is present, $Y|H_1 = \sum_{i=1}^{N} s_i + \sum_{i=1}^{N} n_i \sim \mathcal{N}\left(\mu+S, \sigma^2\right)$. Hence, $p(Y|H_0) = \phi(Y|\mu, \sigma^2)$ and $p(Y|H_1) = \phi(Y|\mu + S, \sigma^2)$, where $\phi(x|\mu, \sigma^2)$ is the PDF of the normal distribution $\mathcal{N}(\mu, \sigma^2)$, *i.e.*, $\phi(x|\mu, \sigma^2) = \frac{1}{\sqrt{2\pi}\sigma} \exp\left(-\frac{(x-\mu)^2}{2\sigma^2}\right)$. Therefore, the likelihood ratio is $\frac{p(Y|H_1)}{p(Y|H_0)} = \exp\left(\frac{(2Y-2\mu-S)S}{2\sigma^2}\right)$ and the likelihood ratio test becomes the rule in (2).